Valence-band density of states of near-noble-metal (Ni,Pd,Pt) monosilicides by using soft-x-ray-emission spectroscopy

S. Yamauchi*
Reserach Laboratories, Nippondenso Co., Ltd., Nissin-cho, Aichi, 470-01, Japan

S. Kawamoto,† M. Hirai, M. Kusaka, and M. Iwami
Research Laboratory for Surface Science, Faculty of Science, Okayama University, Okayama 700, Japan

H. Nakamura
Osaka Electro-Communication University, Hatsu, Neyagawa, Osaka 572, Japan

H. Ohshima and T. Hattori
Research Laboratories, Nippondenso Co., Ltd., Nissin-cho, Aichi, 470-01, Japan
(Received 28 March 1994; revised manuscript received 29 June 1994)

We have focused our attention on the valence-band density of states (VB-DOS) of near-noble-metal monosilicides (NiSi, PdSi, and PtSi) from the study of soft-x-ray-emission spectroscopy. These three silicides have several similarities, i.e., electron configuration for each metal atom and crystallographic structure of each silicide. However, the spectral shape of the Si $L_{2,3}$ emission, which has information of the Si s and/or the d VB-DOS, of each silicide has indicated the clear differences from each other. Moreover, it is shown that these characteristics are closely related to the features observed in the Si p state derived from Si $K\beta$ emission spectra. From the spectral analysis related to the energy difference between Si p bonding and antibonding states considering the interaction strength of the Si p-metal d of each silicide, the influence of Si-Si interatomic distance on the value of the full width at half maximum of the Si s bonding state and the Si s and/or d contribution on the upper part of the VB-DOS structure, we have suggested a valence-band structure of near-noble-metal monosilicides.

I. INTRODUCTION

Soft-x-ray-emission band spectra of Si in metal silicides provide useful information on a valence-band density of states (VB-DOS), which includes a partial projection of the electronic structure of metal silicides. The study of metal silicide by using conventional photoelectron spectroscopy gives a picture of the total VB-DOS below the Fermi level. On the other hand, soft-x-ray-emission spectra, i.e., Si $L_{2,3}$ and Si $K\beta$, give more detailed information because of their site and symmetry selectivity; they relate directly to the partial VB-DOS on the Si atoms.[1] In many reports,[2] it has been considered to be confirmed that the structure of the VB-DOS of metal silicides is as follows. (a) The upper part of the valence band is mainly constructed by the Si p and metal d bonding and antibonding states. (b) The lower part of the valence band is formed by the nonbonding Si s state. However, several recent observations using the study of soft-x-ray emission suggest that the Si s and/or the d states extend to the upper part of the valence band.[3-10] Therefore, the observation of the partial VB-DOS is necessary for us to discuss the VB-DOS of a metal silicide.

In this study, we have focused our attention on the VB-DOS of near-noble-metal (Ni,Pd,Pt) monosilicides examined by soft-x-ray-emission spectroscopy (SXES). These metal atoms have the same electron configuration on each d orbital, i.e., Ni:$3d$,[10] Pd:$4d$,[10] and Pt:$5d$.[10] Moreover, NiSi, PdSi, and PtSi have more interesting similarity in the crystal structure. Each silicide has an orthorhombic MnP structure, which has the same coordination number, and the lattice parameters are almost comparable to each other as shown in Table I. Therefore, the comparison of the VB-DOS for these silicides will give important information on the valence-band structure of a metal silicide.

TABLE I. The lattice parameters of orthorhombic near-noble-metal monosilicides (NiSi, PdSi, and PtSi).

	Lattice parameter (nm)			
	a	b	c	Ref.
NiSi	0.5233	0.3258	0.5659	11
PdSi	0.5599	0.3381	0.6133	12
PtSi	0.5595	0.3603	0.5939	12

II. EXPERIMENT

Near-noble-metal monosilicide samples were prepared by an ordinary solid phase reaction on single-crystal Si substrates. After degreasing of the Si substrate in organic solvents, and removing an oxide layer in buffered HF, each metal layer, i.e., Ni, Pd, and Pt, was deposited in a vacuum chamber with the pressure of $\sim 10^{-6}$ Pa by eva-

poration. The metal (film ~100 nm)/Si (substrate) samples were heat treated in an electric furnace under N_2 and/or H_2 gas flow. A film thickness of deposited metal was estimated by the formed silicide thickness. In order to obtain the single-phase silicide layer, the heat-treatment temperature for each metal silicide was selected as follows: NiSi, 600 °C; PdSi, 900 °C; and PtSi, 700 °C. The growth of each near-noble-metal monosilicide film was ascertained by x-ray diffraction analysis.

SXES experiments were carried out by means of an x-ray spectrometer,[13] which consists of an electron gun, a grating monochromator, a crystal monochromator, an exit slit, an x-ray detector, and a sample stage. The gold-coated grating monochromator was set on a Rowland circle. The incident electron beam energies E_p were controlled between 0.5 and 30.0 keV, where the beam diameter was ~1 μm. The incident electron beam energy was controlled for the x-ray production region to be only in the silicide layer. We measured several SXES spectra for near-noble-metal monosilicides, i.e., Si $L_{2,3}$, Si $K\beta$, and Si $K\alpha$ emission. Si $L_{2,3}$ and $K\beta$ emission band spectra have given the VB-DOS information of each silicide. Si $K\alpha$ emission, i.e., core transitions, have been used for the determination of the Fermi level E_F on each spectra.

III. RESULTS

Si $K\beta$ and Si $L_{2,3}$ emission band spectra for NiSi, PdSi, and PtSi are shown in Figs. 1 and 2, respectively. It should be noted that each spectrum has two prominent peaks as designated by Ai, Bi, Ci, and Di. We will come back to this point later.

IV. DISCUSSION

A. Comparison with existing theoretical study

For the sake of discussion, in Figs. 3, 4, and 5, the Si $K\beta$ emission spectra [Figs. 3(a), 4(a), and 5(a)], and the Si $L_{2,3}$ emission spectra [Figs. 3(b), 4(b), and 5(b)], are shown in comparison with proposed theoretical partial VB-DOS's, i.e., the Si s,p contribution [Figs. 3(c), 4(c), and 5(c)] for NiSi, PdSi, and PtSi, respectively, where the adopted theoretical method is the iterative extended Huckel theory (IEHT).[12] Each SXES spectrum is subjected to linear background substraction and normalized at the maximum intensity. The abscissa is scaled by the binding energy on the basis of the Fermi level, which is set using the Si $K\beta$ and Si $K\alpha$ emission and the binding energy of the Si $2p$ core level determined by x-ray photoemission spectroscopy (XPS).[14]

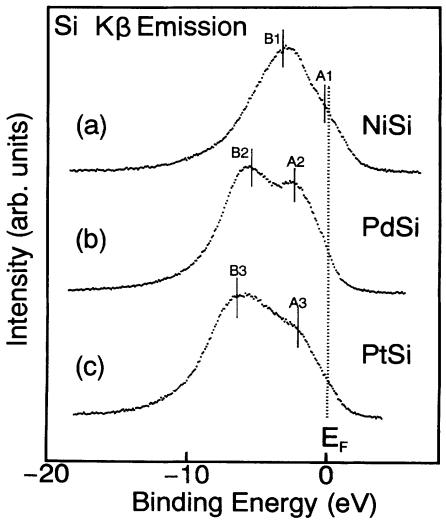

FIG. 1. Si $K\beta$ emission spectra of near-noble-metal monosilicides (a) NiSi, (b) PdSi, and (c) PtSi.

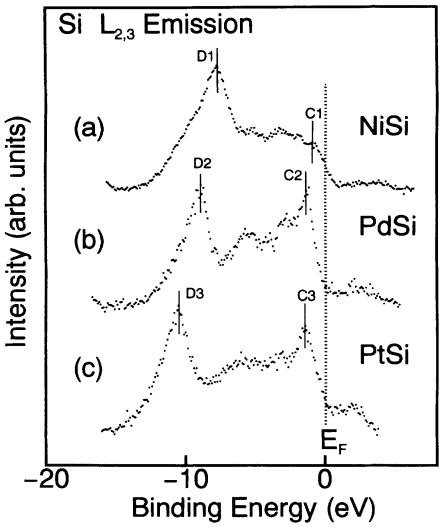

FIG. 2. Si $L_{2,3}$ emission spectra of near-noble-metal monosilicides (a) NiSi, (b) PdSi, and (c) PtSi.

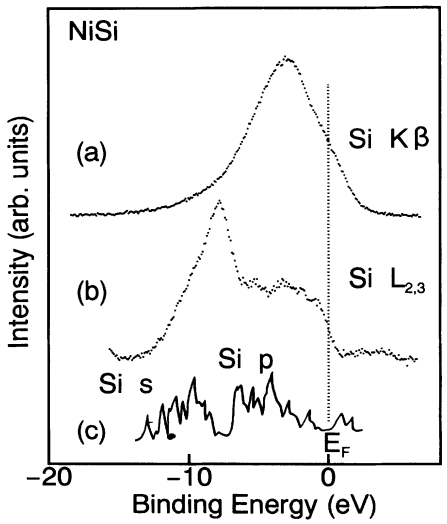

FIG. 3. Soft-x-ray emission spectra of NiSi, i.e., (a) Si $K\beta$ emission and (b) Si $L_{2,3}$ emission. (c) is the theoretical partial VB-DOS (Ref. 12).

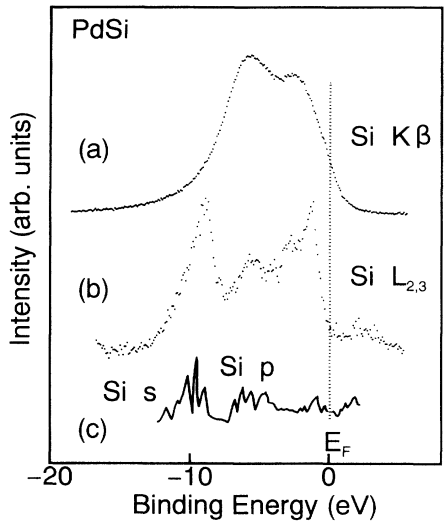

FIG. 4. Soft-x-ray-emission spectra of PdSi, i.e., (a) Si $K\beta$ emission and (b) Si $L_{2,3}$ emission. (c) is the theoretical partial VB-DOS (Ref. 12).

The SXES spectra of the NiSi, Si $K\beta$ emission spectrum [Fig. 3(a)], which reflects the partial VB-DOS with Si p symmetry, has the following features: (a) a broad peak at binding energy $E_b \sim -3$ eV, and (b) a small shoulder near the Fermi level. These structures are considered to be caused by the Si p state due to Si p and Ni d bonding and antibonding states in the valence band. It seems that the theoretical prediction for the Si p VB-DOS [Fig. 3(c)] cannot explain very well the present experimental results, especially, the double-peaked structure below the Fermi level, which has been shown in Fig. 1(a), and does not appear in Fig. 3(c). Such disagreement will be discussed in the last part of this section. The Si $L_{2,3}$ emission spectrum of NiSi [Fig. 3(b)] shows several characteristics as follows: (c) a prominent peak at $E_b \sim -8$ eV, and (d) a terrace from $E_b \sim -6$ to -0.5 eV. The theoretical Si s state is almost coincident with feature (c) above of the experimental Si $L_{2,3}$ emission spectra, where they have a small difference in the binding energy. However, this theoretical prediction tells nothing about the terrace observed in the Si $L_{2,3}$ emission spectrum, feature (d) above, which is considered to correspond to the upper part of the valence band of NiSi.

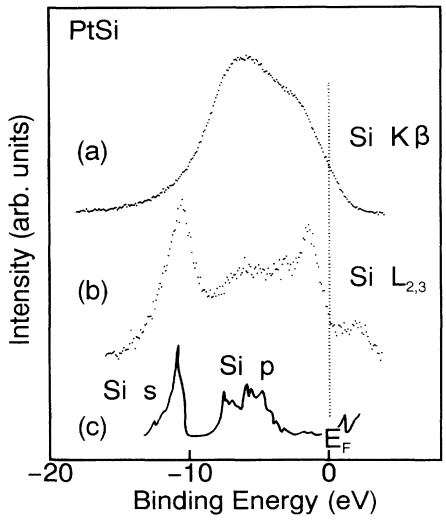

FIG. 5. Soft x-ray emission spectra of PtSi, i.e., (a) Si $K\beta$ emission and (b) Si $L_{2,3}$ emission. (c) is the theoretical partial VB-DOS (Ref. 12).

In Fig. 4, the theoretical partial VB-DOS of PdSi is shown for discussion. The Si $K\beta$ emission spectrum [Fig. 4(a)] shows a double-peaked structure, whose peak positions are at $E_0 \sim -5.5$ and -2.5 eV. This feature is considered to indicate clearly that the Si p VB-DOS splits due to the Si p–Pd d bonding and antibonding structure. The energy position of the theoretical partial VB-DOS of Si p symmetry [Fig. 4(c)] corresponds almost to Si p bonding structure derived by this Si $K\beta$ emission. However, the double-peaked structure does not clearly appear in the theoretical VB-DOS of Fig. 4(c). This difference will also be discussed in the last part of this section. The Si $L_{2,3}$ emission spectrum of PdSi [Fig. 2(b)] has the following features: (e) a prominent peak at $E_b \sim -9$ eV, (f) a terrace at $E_b = -2$ to -7 eV with a small peak at $E_b \cong -5.5$ eV, and (g) another peak at $E_b \sim -1$ eV. It can be concluded that the prominent peak at E_b to -9 eV, feature (e) above, reflects the partial VB-DOS of the Si s bonding states, which coincides with the theoretical observation, Fig. 4(c). The signal of the terrace and the small peak at $E_b = -2$ to -7, feature (f) above, is due to the superposition of the Si $L_{2,3}$ emission and the third-order line of Pd $L\xi_1$ emission.[8] However, the origin of the signal at the middle and upper part of the Si $L_{2,3}$ emission, i.e., the signal around the peak at $E_b \simeq -1$ eV, is not clear. The theoretical calculation [Fig. 4(c)] shows the nonexistence of Si s states in the upper part of the VB-DOS.

The VB-DOS of PtSi has meaningful features as can be seen in Fig. 5. The Si $K\beta$ emission spectrum [Fig. 5(a)] shows a broad peak at $E_b \sim -7$ eV and a shoulder at $E_b \sim -2$ eV. These features can again be referred to the Si p VB-DOS due to the Si p–Pt d bonding and antibonding states. The peak position of theoretical partial VB-DOS of Si p symmetry also corresponds to the Si p bonding structure explored by this Si $K\beta$ emission. However, the theoretical prediction is not enough to explain the shoulder structure, i.e., Si p–Pt d antibonding state. Such disagreement will also be discussed in the last part of this section. The Si $L_{2,3}$ emission spectrum of PtSi [Fig. 5(b)] has interesting features, described as follows: (h) a prominent peak at $E_b \cong -11$ eV, (i) a terrace at $E_b = -2$ to -9 eV, and (j) another peak at $E_b \sim -1$ eV. It can be concluded that the prominent peak at $E_b \sim -11$ eV, feature (h) above, mainly reflects the partial VB-DOS of Si s bonding states, which agrees with the theoretical observation [Fig. 5(c)]. However, the origin of the signal at the middle and upper part of the Si $L_{2,3}$ emission, i.e., $E_b = 0$ to -9 eV, is again not clear. The theoretical cal-

culation [Fig. 5(c)] is not able to explain the existence of Si s and/or d states in the upper part of the VB-DOS.

Considering the differences between the SXES spectra and the theoretical VB-DOS of three silicides, we should discuss the discrepancy between the experimental results and the theoretical calculation. The Si $K\beta$ emission spectra, which reflect the partial VB-DOS of Si p states, i.e., Si p bonding and antibonding states, correspond well with other experimental results, i.e., SXES (Ref. 15) and XPS (Ref. 16). The theoretical calculation using the augmented plane wave (APW) method has shown a good agreement with the experimental Si $K\beta$ emission spectra of Ti, Cr, Co, and Ni silicides,[5] except for the slight difference depending on the self-energy effects. Therefore, it is considered that the IEHT calculation is not able to explain all of the partial VB-DOS structure of metal silicides. Especially, the upper part of the VB-DOS structure derived by Si $L_{2,3}$ emission has never been predicted by the IEHT calculation. Although the APW calculation has shown the existence of Si d states near the Fermi level in the case of several metal silicides, the VB-DOS's of three near-noble-metal monosilicides have not yet been clarified. The VB-DOS structure of these silicides will be discussed systematically in the following section.

B. Energy difference between bonding and antibonding states of Si p partial VB-DOS

The partial VB-DOS of each near-noble-metal monosilicide has the information useful in interpreting the detailed structure of its valence band. The study of the Si $K\beta$ emission spectrum, as discussed above, gives information on the Si p bonding and antibonding states due to Si p–metal d bond formation, which is in agreement with what has been believed so far.[8,10,15,16] In this section we have mainly paid attention to the Si p–metal d bonding states of near-noble-metal monosilicides from the viewpoint of energy difference between bonding and antibonding: $E_{B/A}$.

Figure 1 shows the comparison of the Si $K\beta$ emission spectra of three near-noble-metal monosilicides. In this figure, the Si p bonding and antibonding states for each silicide are indicated by the vertical solid lines which designate the bonding states ($B1$–$B3$) and antibonding states ($A1$–$A3$). The energy position of each state is calculated by a spectral deconvolution assuming each peak is a Gaussian function. It has been considered that the energy difference between the Si p bonding and antibonding states $E_{B/A}$ directly depends on the interaction strength of the Si-metal atom bonding.[16] In Fig. 6, $E_{B/A}$ of three silicides measured by the Si $K\beta$ emission spectra are plotted in comparison with the results of either SXES (Ref. 15) or XPS (Ref. 16) where the $E_{B/A}$ values measured by the SXES study are almost in agreement with those of previous reports.[15,16] The abscissa of Fig. 6 shows the heats of formation (kcal/metal atom): $-dH_f$,[17] which describes the thermodynamical measure of the bonding strength of each silicide. The value of $E_{B/A}$ increases with the increase of the heat of formation, which shows that $E_{B/A}$ depends on the bonding strength.

Next, we have tried an estimation of the interaction

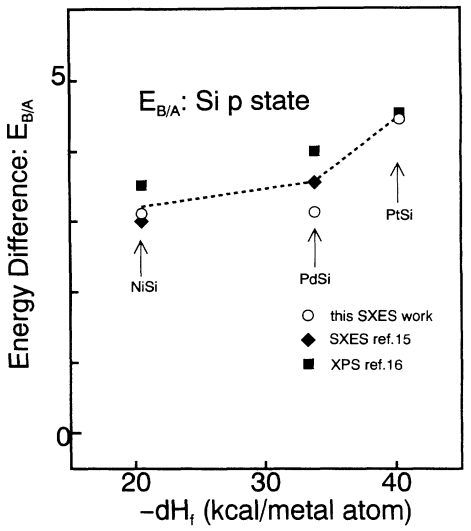

FIG. 6. The energy differences $E_{B/A}$ for the Si p state between bonding and antibonding states of near-noble-metal monosilicides as a function of the heats of formation of silicides.

strength of Si p–metal d bonding by calculating the following interatomic matrix element: V_{ldm}, which is produced by the transition-metal pseudopotential theory,[18]

$$V_{\mathrm{ldm}}=\eta_{\mathrm{ldm}}\frac{\hbar^2}{m}\frac{r_d^{3/2}}{d^{7/2}} . \tag{1}$$

$V_{pd\sigma}$ and $V_{pd\pi}$ which reflect the interaction strength of Si p–metal d bonding and antibonding, respectively, are given by the constants $\eta_{pd\sigma}(=-2.95)$ and $\eta_{pd\pi}(=1.36)$ obtained from Mattheiss's APW calculation. r_d is the metal d-orbit radius and d is the nearest-neighboring Si-metal atom distance. Table II shows the several parameters and calculated interatomic matrix elements, i.e., $V_{pd\sigma}$, $V_{pd\pi}$, and $\Delta V(=V_{pd\pi}-V_{pd\sigma})$, of three near-noble-metal monosilicides. $V_{pd\sigma}$ of each silicide indicates the interaction strength, which corresponds almost to the heat of formation. The behavior of ΔV also shows an agreement with that of the energy difference $E_{B/A}$ deduced from the Si $K\beta$ emission spectra of three silicides. Considering the experimental results and theoretical calculation, it can be said that there is a close relationship between the energy difference $E_{B/A}$ and the interaction strength of Si p–metal d bonding.

TABLE II. The calculated interatomic matrix elements using Eq. (1); $V_{pd\sigma}$, $V_{pd\pi}$, and $\Delta V(=V_{pd\pi}-V_{pd\sigma})$. For r_d and d, see text.

	r_d (nm)	d (nm)	$V_{pd\sigma}$	$V_{pd\pi}$	$\Delta V(=V_{pd\pi}-V_{pd\sigma})$
NiSi	0.071	0.2334	−0.692	0.319	1.011
PdSi	0.094	0.2487	−0.845	0.389	1.234
PtSi	0.104	0.2510	−0.952	0.439	1.391

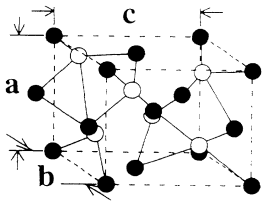

FIG. 7. The crystallographic model of MnP structure. ● and ○ indicate the metal (Ni, Pd, and Pt) and Si atoms, respectively.

C. Relationship between the partial VB-DOS for each near-noble-metal monosilicide and the Si-Si interatomic distance

The three silicides have similar crystallographic properties, i.e., the same crystal structure (MnP structure), the same number of coordination, etc. Therefore, the interatomic distance between neighboring atoms should have an important effect on the VB-DOS in the silicide structure. Table III(a) lists the average interatomic distances between the Si and Si atom, d[Si-Si], between the Si and metal atom, d[Si-M], and between the metal and metal atom, d[M-M], in the unit cell of each silicide. Figure 7 shows the unit cell of MnP structure. Table III(b) shows d[M-M] in each pure metal. One can see that the d[M-M] in each pure metal, which directly reflects the atomic radius of each metal atom, has a certain correlation with d[Si-M] and d[M-M] in three silicides. In addition, d[Si-Si] is affected by the atomic size of metal element, i.e., Ni, Pd, and Pt, in the near-noble-metal monosilicides. Therefore, we will try to discuss the relationship between the Si s derived VB-DOS of the metal silicides and the interatomic distances.

Figure 8 shows the relationship between d[Si-Si] and the full width at half maximum (FWHM) value of the Si s bonding states, FWHM [Si s], i.e., those of $D1$–$D3$ in Fig. 2. The values of FWHM [Si s] are directly measured on the Si $L_{2,3}$ emission spectra of three silicides. The FWHM [Si s], which is considered to relate directly to d[Si-Si] in each silicide, shows the clear difference among

TABLE III. (a) Interatomic distances d (nm) between each element for three near-noble-metal monosilicides and (b) nearest interatomic distance of the metal-metal atom for each pure metal.

	(a)		
	NiSi	PdSi	PtSi
d[Si-Si]	0.347 8	0.369 9	0.374 1
d[Si-M]	0.233 4	0.248 7	0.251 0
d[M-M]	0.284 7	0.302 0	0.307 3
	(b)		
	Ni	Pd	Pt
d[M-M]	0.249 17	0.275 05	0.277 41

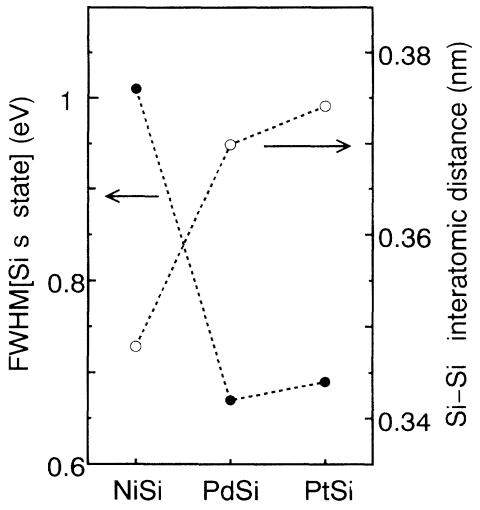

FIG. 8. The relationship between the interatomic distances of Si-Si, d[(Si-Si)], and the FWHM value of Si s bonding states, FWHM [Si s], of three near-noble-metal monosilicides.

three near-noble-metal monosilicides. The FWHM [Si s] value for NiSi is considerably larger than those of PdSi and PtSi, which can be explained as follows. The strength of the Si-Si bonding is considered to increase with decreasing d[Si-Si], which enhances the amount of the wave-function overlap of the Si s states to result in the increase in the FWHM [Si s] in NiSi. On the other hand, for PdSi and PtSi, the difference in d[Si-Si] is not remarkable, which is consistent with the fact that the FWHM [Si s] values are almost the same. Such an identical situation for PdSi and PtSi will be the origin of the similarity in the Si $L_{2,3}$ emission spectra [Figs. 2(b) and 2(c)].

D. The origin of the upper part of VB-DOS explored by Si $L_{2,3}$ emission

Si $L_{2,3}$ emission spectra of three near-noble-metal monosilicides are compared in Fig. 2. According to the Si $L_{2,3}$ emission band spectra for the silicides, it can be said that there is a great difference between the one for NiSi and those for PdSi and PtSi, especially on the upper part of the valence band. Though several SXES reports on Si $L_{2,3}$ emission bands have appeared to consider contribution of Si s and/or d states to the VB-DOS by the dipole selection rule,[3] the clear explanation of the origin of the upper part of the VB-DOS structure has only been reported for several limited metal silicides.[3–7,10] Except for $NiSi_2$ which has been explained as a Si s antibonding state existing near the Fermi level,[3,4] the upper part of VB-DOS's of several other silicides are explained by the existence of Si d states which are formed by the bonding state with the metal d orbital. An earlier report[5] has indicated that such a Si d contribution is in some way linked to the diffuse nature of metal d states which could lead to enhanced tailing onto the Si site. In general, the metal d character becomes more remarkable with in-

creasing size of the metal d orbital.

Near-noble-metal monosilicides constitute a typical system, where sizes of metal d orbitals are different. The upper-part structure of the VB-DOS becomes more remarkable with increasing size of the metal d orbital from NiSi to PtSi through PdSi. This behavior may indicate that the upper part of the VB-DOS's of three silicides derived from Si $L_{2,3}$ emission are constructed by bonding with the metal d state. Comparing the theoretical predictions of Si d contribution as the bonding state with metal d state in other silicides, we consider that the relative weight of the Si d state to bonding is large. However, the role of the Si s state in bonding with metal d is unclear for near-noble-metal monosilicides. Further (theoretical) studies will help the full understanding of the Si $L_{2,3}$ emission spectra for the near-noble-metal monosilicides.

V. SUMMARY

In this study, we have tried to clarify the VB-DOS of NiSi, PdSi, and PtSi. These three silicides have quite similar properties, i.e., the crystal structures and the electron configurations of metal elements are similar. We suggest the structure of the VB-DOS's of near-noble-metal monosilicides, i.e., NiSi, PdSi, and PtSi, using Si $K\beta$ and $L_{2,3}$ SXES experiments data, whose properties were not able to be explained quite well by previously reported theoretical calculation. The features of VB-DOS of each silicide have been explained as follows.

(1) Si $K\beta$ emission spectra of three silicides have clearly shown on the Si p bonding and antibonding states, of which energy difference is concluded to depend on the heat of formation, $-dH_f$, of the silicides. The $-dH_f$ is clarified to relate closely to the interaction strength of each Si-metal atom bonding. Such a property is almost in agreement with theoretical calculation.

(2) The interatomic distances of Si-Si, d[Si-Si], have a significant relationship with the wave-function overlap of the Si s bonding state. The increase of FWHM [Si s] bonding state with decreasing d[Si-Si] indicates that the d[Si-Si] gives the influence on the spread of Si s related VB-DOS in energy.

(3) It is derived from the Si $L_{2,3}$ emission that the increase of the Si s and/or d derived VB-DOS of the silicides at the upper part is closely related with the increase in the size of the metal d orbital. The VB-DOS's are considered to be constructed by the bonding state, i.e., Si s and/or d, with metal d state.

ACKNOWLEDGMENTS

The authors would like to express their sincere thanks to Dr. G. Tsuzuki (Research Laboratories Nippondenso Co., Ltd.) for his valuable comments. This work was partly supported by Scientific Grant-in-Aid No. 05555191, from the Ministry of Education, Science, and Culture.

*Author to whom all correspondence should be addressed.
†Present address: Tamano Laboratory, Mitsui Engineering & Shipbuilding Co., Ltd., Tamano, Okayama 706, Japan.

[1]G. Wiech, in *Soft X-ray Band Spectra and the Electronic Structure of Metals and Materials*, edited by D. J. Fabian (Academic, New York, 1968), p. 59.
[2]See, for example, G. W. Rubloff, Surf. Sci. **132**, 268 (1983).
[3]H. Nakamura, M. Iwami, M. Hirai, M. Kusaka, F. Akao, and H. Watabe, Phys. Rev. B **41**, 12 092 (1990).
[4]J. J. Jia, T. A. Callcott, W. L. O'Brien, Q. Y. Dong, J.-E. Rubensson, D. R. Mueller, D. L. Ederer, and J. E. Rowe, Phys. Rev. B **43**, 4863 (1991).
[5]P. J. W. Weijs, H. van Leuken, R. A. de Groot, J. C. Fuggle, S. Reiter, G. Wiech, and K. H. J. Buschow, Phys. Rev. B **44**, 8195 (1991).
[6]H. Nakamura, M. Hirai, M. Kusaka, M. Iwami, and H. Watabe, J. Phys. Soc. Jpn. **61**, 616 (1992).
[7]J. J. Jia, T. A. Callcott, W. L. O'Brien, Q. Y. Dong, D. R. Mueller, D. L. Ederer, Z. Tan, and J. I. Budnick, Phys. Rev. B **46**, 9446 (1992).
[8]S. Kawamoto, M. Hirai, M. Kusaka, H. Nakamura, M. Iwami, and H. Watabe, Jpn. J. Appl. Phys. **32**, L597 (1993).
[9]V. R. Galakhov, E. Z. Kurmaev, S. N. Shamin, L. V. Elokhina, Yu. M. Yarmoshenko, and A. A. Bukharaev, Appl. Surf. Sci. **72**, 73 (1993).
[10]S. Yamauchi, M. Hirai, M. Kusaka, K. Iwami, H. Nakamura, H. Ohshima, and T. Hattori, Jpn. J. Appl. Phys. **33**, L1012 (1994).
[11]F. d'Heurle, C. S. Petersson, J. E. E. Baglin, S. J. LaPlaca, and C. Y. Wong, J. Appl. Phys. **55**, 4208 (1984).
[12]O. Bisi and C. Calandra, J. Phys. C **14**, 5479 (1981).
[13]M. Iwami, M. Hirai, M. Kusaka, M. Kubota, S. Yamamoto, H. Watabe, M. Kawai, and H. Soezima, Jpn. J. Appl. Phys. **29**, 1353 (1990).
[14]P. J. Grunthaner, F. J. Grunthaner, and A. Madhukar, J. Vac. Sci. Technol. **20**, 680 (1982).
[15]K. Tanaka, T. Saito, K. Suzuki, and R. Hasegawa, Phys. Rev. B **32**, 6853 (1985).
[16]P. J. Grunthaner, F. J. Grunthaner, and A. Madhukar, Physica **117&118B**, 831 (1983).
[17]G. V. Samsonov and I. M. Vinitskii, *Handbook of Refractory Compounds* (IFI/Plenum, New York, 1980).
[18]W. A. Harrison, *Electronic Structure and the Properties of Solids* (Freeman, San Francisco, 1980).
[19]M. Kasaya, S. Yamauchi, M. Hirai, M. Kusaka, M. Iwami, H. Nakamura, and H. Watabe, J. Phys. Soc. Jpn. (to be published).